Hindawi
Shock and Vibration
Volume 2021, Article ID 7565004, 16 pages
https://doi.org/10.1155/2021/7565004

Research Article

A New Method for Controlling Rockbursts in the Mining Roadway of Ultrathick Coal Seams Based on the Dual Pressure Relief Method

Guangyuan Yu,[1,2] **Jiong Wang**,[1,2] **Zimin Ma**,[3] **Wei Ming**,[1,2] **and Xingen Ma**[1,4,5]

[1]*State Key Laboratory for Geomechanics and Deep Underground Engineering, China University of Mining and Technology, Beijing 100083, China*
[2]*School of Mechanics and Civil Engineering, China University of Mining and Technology, Beijing 100083, China*
[3]*School of Resources and Environmental Engineering, Shandong University of Technology, Zibo 255000, China*
[4]*Huaneng Coal Technology Research CO, LTD, Beijing 100070, China*
[5]*Coal Burst Research Center of China Jiangsu, Xuzhou 221000, China*

Correspondence should be addressed to Jiong Wang; wangjiong0216@163.com and Xingen Ma; 294185559@qq.com

Received 20 July 2021; Accepted 19 August 2021; Published 29 August 2021

Academic Editor: Zonglong Mu

To control rockbursts in mining roadways in ultrathick coal seams, a new method for preventing rockbursts through dual pressure relief by roof cutting through cumulative blasting in medium-deep boreholes from the conveyor gateway and return airway was proposed. The mechanical characteristics of key overlying strata of the working face under the effect of dual pressure relief were theoretically investigated. Furthermore, a mathematical relationship between the roof-cutting depth and the advanced abutment pressure on the working face was established to reveal the mechanism of dual pressure relief in controlling rockbursts. Moreover, the effect of the dual pressure relief method on controlling rockbursts was validated through numerical simulation and field testing. Results showed that artificially increasing the caving height of gangues in goaf based on the dual pressure relief method can restrict the subsidence of key strata, thus reducing the advanced abutment pressure of the working face; the method influences a range of 20 m in front of the working face along the strike and areas 30 m away from the two roadways along the dip. The average energy density of coal in the side of the conveyor gateway is decreased by 15.4%, while that in the side of return airway is reduced by 13.8% within the range of influence. The field test results indicated that the average pressure on support declines by 21.4% within 30 m from the working face to the conveyor gateway, while it decreases by 20.5% within that region 25 m from the return airway by using the dual pressure relief method. After conducting dual pressure relief, the total number of microseismic (MS) events during mining of the working face is decreased by 25.4%. The number of MS events with energy release exceeding 10^3 J falls by 36.6%, while the number of events releasing less than 10^3 J is increased by 28.6%. The characteristics of MS energy release change from coexistence of low-energy events and a small number of high-energy events to the occurrence of numerous low-energy events. Results can verify the effectiveness of the dual pressure relief method in controlling rockbursts in the mining roadway of ultrathick coal seams.

1. Introduction

A rockburst is a common dynamic disaster that is often accompanied by the sudden or violent ejection of coal or rock during the exploitation of underground resources [1, 2]. In recent years, both the number of mines prone to rockburst and the intensity and frequency of rockbursts in China have been constantly increasing with the growth of the mining depth [3, 4]. Rockbursts often occur in a complex manner under particular conditions and sometimes occur without warning [5]. Rockbursts tend to cause large-area collapse of the roadway, casualties, and equipment damage and induce some secondary disasters such as gas outbursts, thus greatly restricting the safe operation of a mine [6, 7].

Given that rockbursts mainly occur in the mining roadway, the control over rockbursts in the mining roadway has become a focus of much research [8]. Pan et al. [9] proposed a method for releasing pressure through deep-hole interval blasting. The degree of energy concentration in the interval of rockburst start-up declines after performing interval blasting, thus hindering the initiation of a rockburst. Zhang et al. [10] found that water injection into coal seams can reduce the strength and brittleness of coal, thus decreasing the risk of an outburst, thus preventing a later rockburst. Qi et al. [11] found that break-tip blasting in deep holes can fundamentally change the stress distribution in the coal rock and significantly reduce the stress within the effective blasting range. Furthermore, they proposed a method for controlling rockburst by using break-tip blasting in deep holes. Pan et al. [12] changed the energy released during a rockburst in coal seams by artificially prefabricating defects and aimed at control of the rockburst by forming engineering defect bodies through drilling and blasting. Jiang et al. [13] proposed reducing the overall strength of coal by cutting coal through hydraulic fracturing at a fixed point under ultrahigh pressure to decrease the volume of the energy-storage unit. In this way, the energy-storage capacity of coal is weakened to realize regionally active control of rockburst risk. Ouyang et al. [14] proposed the production of numerous cracks in coal through hydraulic fracturing to reduce the outburst proneness of coal and changes in the rate of release of energy in coal, thus preventing rockbursts. Xia et al. [15] studied the mechanism of hydraulic reaming of gutters in rockburst control in coal seams and proposed the use of a double-hole arrangement groove-groove technique for separating slotted holes and slag-discharging holes; this can significantly reduce the risk of rockburst-induced disasters in mine roadways. Li et al. [16] controlled rockburst triggered by fracture of overlying strata during fully mechanized caving mining by weakening the disturbance induced by mine earthquakes through reasonable presplitting and cutting of the roof. Zhao et al. [17] released high stress accumulated at the floor and coal in sidewalls by deep-hole floor breaking combined with floor-break blasting at the middle part of the floor with that in coal seams, thus alleviating the risk of a rockburst at the floor.

In recent years, scholars have also proposed the method for rockburst control by combining multiple technical schemes aiming at coal seams with strong outburst proneness in complex geological conditions. Dou et al. [18] proposed a comprehensive method for controlling rockburst by combining pressure relief via drilling large-diameter boreholes, directional hydraulic fracturing, and break-tip blasting in deep holes according to the mechanism of rockbursting triggered by superimposing dynamic and static loads. Ouyang [19] demonstrated a pressure relief and rockburst prevention technology with multistage blasting by combining deep-hole roof breaking, floor-break blasting, and pressure relief blasting in coal seams for mines at high risk of rockburst under complex geological and mining conditions. Liu et al. [20] realized the active regional control of rockburst in coal mines by combining fracturing with water injection into coal seams. Pan et al. [21] proposed a method for controlling rockbursts by integrating roof presplit-blasting, pressure relief blasting in coal seams, and floor blasting. They realized the safe mining of a deep working face at high risk of rockbursting. To control rockburst in deep gob-surrounded, irregular coal pillars, Xue et al. [22] developed a rockburst prevention scheme by reducing load and releasing energy from dynamic and static force sources in coal pillars. The scheme combines deep-hole roof blasting and pressure relief through large-diameter borehole drilling in coal, thus avoiding a rockburst. Additionally, some other methods (e.g., the use of segmental hydraulic fracturing at the roof [23] and backfill mining [24]) were also applied for the control of rockburst risk under complex mining conditions.

In the aforementioned schemes, coal rock is weakened by using different technical methods, thus reducing its outburst proneness and transferring stress or releasing strain energy. In this way, a favorable effect was achieved in terms of rockburst control during the mining of thin and medium-thick coal seams; however, different from the mining of thin and medium-thick coal seams, mining of thick and ultra-thick coal seams makes it easier to trigger strong rockbursts due to its characteristics, including a large mining height, stronger mining influence, and larger range of influence [25]. According to statistics, more than 700 rockbursts have happened during the mining of thick coal seams in typical mines in China since 2008 [26]. One or multiple pressure relief schemes were applied in most mines [27]; however, they still failed to effectively control rockburst risk. This result indicated that traditional technical schemes cannot satisfy the requirement for control of rockburst in thick and ultrathick coal seams. Therefore, research into the best method for controlling rockburst on fully mechanized caving mining condition of ultrathick coal seams is regarded as a scientific problem of some urgency.

In view of this, the aims of this study were threefold: (1) A new method for control of rockburst through dual pressure relief by roof cutting through cumulative blasting in medium-deep boreholes in the conveyor gateway and return airway before mining the working face was proposed. Moreover, the mechanism of the dual pressure relief method in rockburst control was elucidated through theoretical analysis. (2) The distribution of the energy in coal in front of the working face under the influence of the dual pressure relief was described through numerical simulation. (3) Through the field test, the characteristics of stratal behaviors and microseismic (MS) events during the mining of the working face under the influence of dual pressure relief were investigated and the effect of the method in controlling rockbursts was verified. The results provide a new direction, and a technical means, for controlling rockburst in the roadways during the mining of ultrathick coal seams.

2. Methods and Technologies

2.1. New Method for Rockburst Control by Dual Pressure Relief

2.1.1. Mechanism of Rockburst Control by Dual Pressure Relief. The method for rockburst control by dual pressure

relief in the roadway during the mining of ultrathick coal seams is summarized as follows: before mining the working face, the mechanical connection between the roadway roof and the roof of goaf is cut as a result of blasting in medium-deep boreholes in the conveyor gateway and return airway (Figure 1(a)). By doing so, the volume of gangues caved in goaf increases. Next, the pressure on coal in front of the working face is reduced by virtue of the filling effect of broken gangues, thus preventing the occurrence of a rockburst.

Only a small volume of gangues cave from the immediate roof after mining under conventional conditions. The caved gangues (after being broken) are not sufficient to backfill the goaf. The overlying strata are subjected to significant rotational subsidence under the effects of gravity and pressure, as shown in Figure 1(b), which causes the pressure on coal ahead of the working face to increase. The increase in the abutment pressure on coal ahead of the working face caused by the subsidence of overlying strata in goaf needs to be alleviated: to this end, the mechanical connection between the roadway roof and the roof of goaf is cut using dual pressure relief to increase the volume of rock caved from the roof in goaf. Due to bulking properties of rock, the increment of the volume of broken rock can compensate for backfill in the goaf when the volume of caved gangues is large enough. In this way, it is possible to support the overlying strata (Figure 1(c)), restrict the speed of movement and settlement of the roof of goaf, change the type of structure of the overlying strata and their mechanism of stress transfer to coal, and weaken the abutment pressure on coal ahead of the working face. Furthermore, the accumulation of energy in coal is reduced, which prevents rockbursts.

2.1.2. Mechanical Model. There are superthick overlying strata on coal seams in deep parts of the mine. Due to differences such as those in lithology, layer thickness, and the load from overlying strata, F-shaped hanging arches with different lengths were formed along the vertical direction at the back of the working face after excavating a coal seam [21]. Under conventional mining conditions, the caving height of the immediate roof in goaf is small and the caved gangues after being broken are insufficient to backfill the goaf. This leaves an unfilled space u with a large height between the F-shape hanging arch above the goaf and gangue piles, whose profile along the strike of the working face (section line A-A′ in Figure 1(b)) is shown in Figure 2(a).

After applying the dual pressure relief technique, the presence of the cut at the roof increases the caving height of the immediate roof in goaf. As a result, the volume of caved gangues increases and thus the caved gangues can be better filled into the goaf after being broken, thus reducing the unfilled space between the hanging main roof and gangue piles, whose profile along the strike of the working face (section line B-B′ in Figure 1(c)) is illustrated in Figure 2(b).

In addition, affected by the mining height, the ultrathick coal seam mining often causes huge mining space, which further intensifies the demand for the volume of caved gangue. Therefore, the influence of mining height should be fully considered. According to the bulking properties of caved gangues and the large mining height, the distance u between gangue piles and the hanging main roof can be calculated using the following formula:

$$u = H_G - H_{c1}(k-1) - \Delta H, \tag{1}$$

where u, H_G, H_{c1}, k, and ΔH refer to the distance between gangue piles and the hanging main roof, the mining height, the caving height of the immediate roof, the bulking coefficient of rock from the immediate roof, and the floor heave of the goaf, respectively.

The hanging arch above the goaf starts to subside slowly under the effects of the load of the overlying strata and the gravity as the working face is excavated, which causes the pressure on coal ahead of the working face to increase rapidly. The main roof will be fractured after it subsides to a certain extent, whose overlying strata still remain in a pseudoplastic state. In this case, a rock beam maintains the force transfer along the advancement direction; one end of this beam is supported by coal in front of the working face and the other end by is supported by gangues in goaf [28], as shown in main roof 2 in Figure 3.

The stronger the outburst proneness of coal samples and the less the initial damage, the larger the storage capacity of elastic strain energy [29]. The coal seams subjected to rockburst tend to exhibit high outburst proneness. The strain energy is stored in that coal ahead of the working face in the form of elastic deformation before rockburst occurs. In this case, the support force provided by the coal increases with increasing deformation; therefore, it is feasible to simplify the immediate roof below the main roof, coal and gangues as elastic media, and the load of overlying strata of the main roof as the uniform load. Therefore, the movement progresses from the main roof subsiding, coming into contact with gangues under the main roof, such that this stabilizing action satisfies the Winkler elastic foundation hypothesis. By taking main roof 2 in Figure 3 as the research object, it is feasible to construct a mechanical model for the main roof after being in contact with gangues, as shown in Figure 4.

According to the Winkler foundation hypothesis, the deflection curve equation for the main roof 2 above the goaf and coal seams was separately established under the coordinate system, as shown in the following formulae:

$$EI\frac{\mathrm{d}^4 w_1(x)}{\mathrm{d}x^4} + k_1\left[w_1(x) - u\right] = q_0, \tag{2}$$

$$EI\frac{\mathrm{d}^4 w_2(x)}{\mathrm{d}x^4} + k_1 w_2(x) = q_0, \tag{3}$$

where E, I, and $\omega(x)$ represent the elastic modulus, moment of inertia, and the deflection of bending and subsidence of the rock beam of the main roof, respectively; k_1 and k_2 separately denote the elastic foundation coefficients of gangue piles and coal seams; u and q_0 refer to the distance

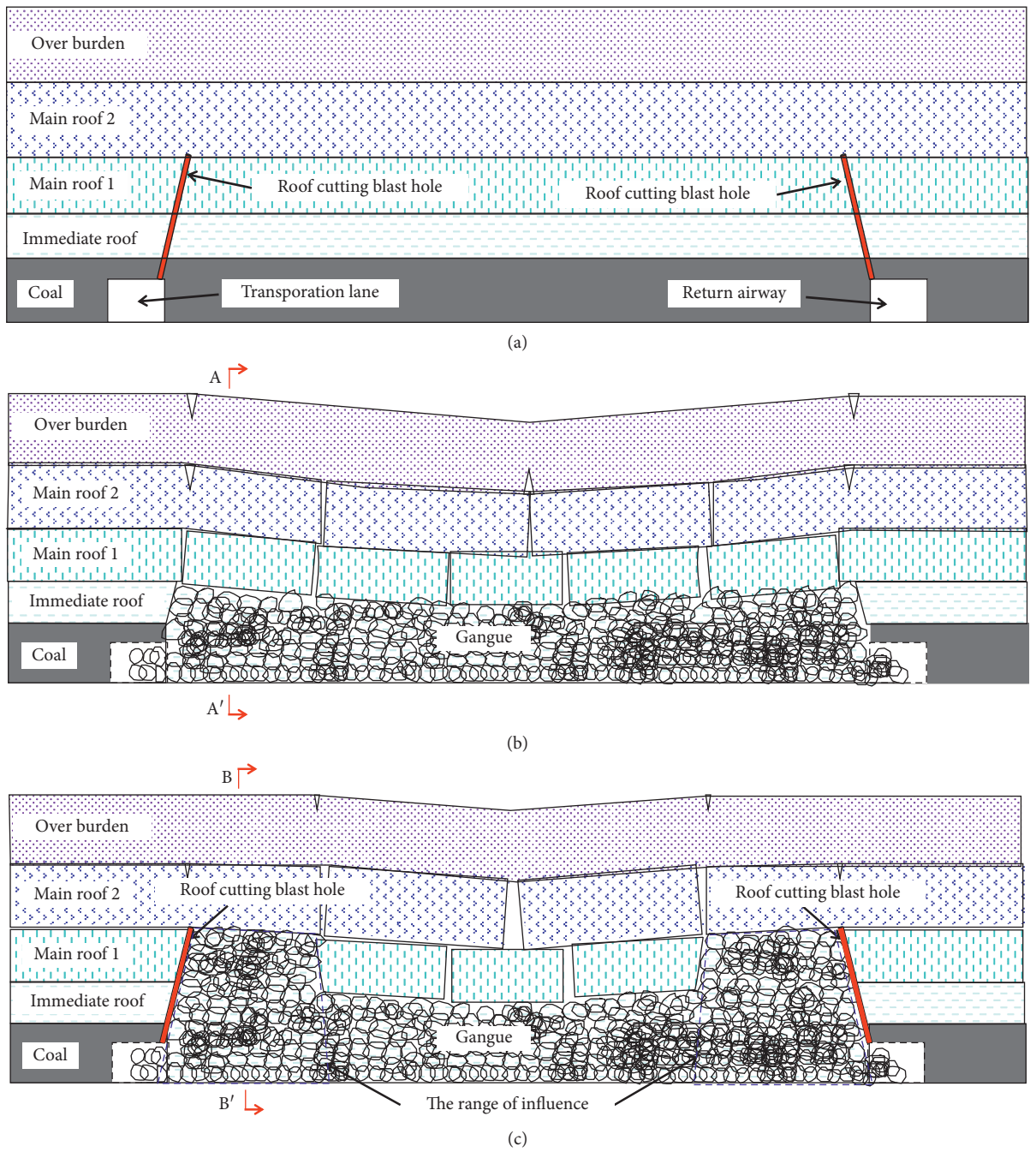

FIGURE 1: The principle of the dual pressure relief technology applied in the mining roadway of ultrathick coal seams. (a) Before mining the working face by using dual pressure relief. (b) Structure of overlying strata after conventional mining of the working face. (c) Structure of overlying strata after mining the working face by using dual pressure relief.

between the gangue piles and main roof and the load of overlying strata of the rock beam of the main roof, respectively.

Assuming that $\beta_1 = \sqrt[4]{k_1/4EI}$ and $\beta_2 = \sqrt[4]{k_2/4EI}$ as well as solving formulae (2) and (3), the deflection curve equations for the main roof 2 above the goaf and coal were determined, as shown in the following formulae:

$$\omega_1 = e^{-\beta_1 x}\left(\frac{\beta_1 - \beta_2}{\beta_1 + \beta_2}\sin\beta_1 x - \cos\beta_1 x\right)\cdot\left(\frac{q_0}{k_1} + u\right) + \frac{q_0}{k_1} + u, \quad (4)$$

$$\omega_2 = e^{\beta_2 x}\left(\frac{\beta_2 - \beta_1}{\beta_1 + \beta_2}\sin\beta_2 x + \cos\beta_2 x\right)\cdot\left(\frac{q_0}{k_1} + u\right)\cdot\frac{\beta_1^2}{\beta_2^2} + \frac{q_0}{k_2}. \quad (5)$$

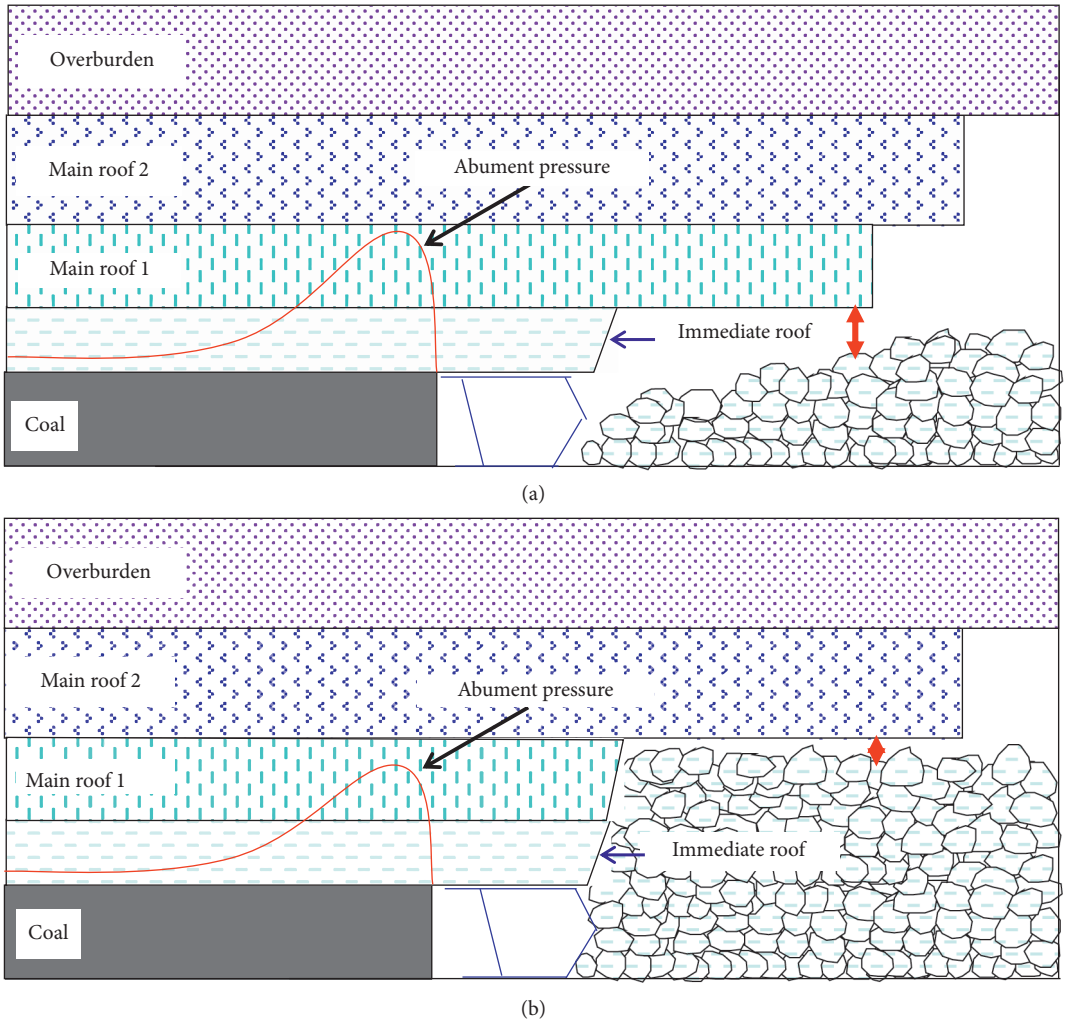

Figure 2: Structure of overlying strata early in the mining of the working face. (a) Conventionally mined working face. (b) The working face subjected to dual pressure relief.

Therefore, the pressures p_1 and p_2 applied by the main roof 2 on gangues in goaf and coal were separately calculated as follows:

$$p_1(x) = k_1 e^{-\beta_1 x}\left(\frac{\beta_1 - \beta_2}{\beta_1 + \beta_2}\sin\beta_1 x - \cos\beta_1 x\right)\cdot\left(\frac{q_0}{k_1} + u\right) + q_0, \tag{6}$$

$$p_2(x) = k_2 e^{\beta_2 x}\left(\frac{\beta_2 - \beta_1}{\beta_1 + \beta_2}\sin\beta_2 x + \cos\beta_2 x\right)\cdot\left(\frac{q_0}{k_1} + u\right)\cdot\frac{\beta_1^2}{\beta_2^2} + q_0. \tag{7}$$

As shown in formula (7), on premise of keeping the main roof in a pseudoplastic state and at same burial depth and geological conditions, the pressure p_2 applied by the main roof 2 on coal ahead of the working face is mainly related to distance u between the main roof and gangue piles. Moreover, the pressure rises with the increase of u. By substituting formula (1) into formula (7), the relationship between pressure p_2 on coal ahead of the working face and the caving height of the immediate roof can be obtained:

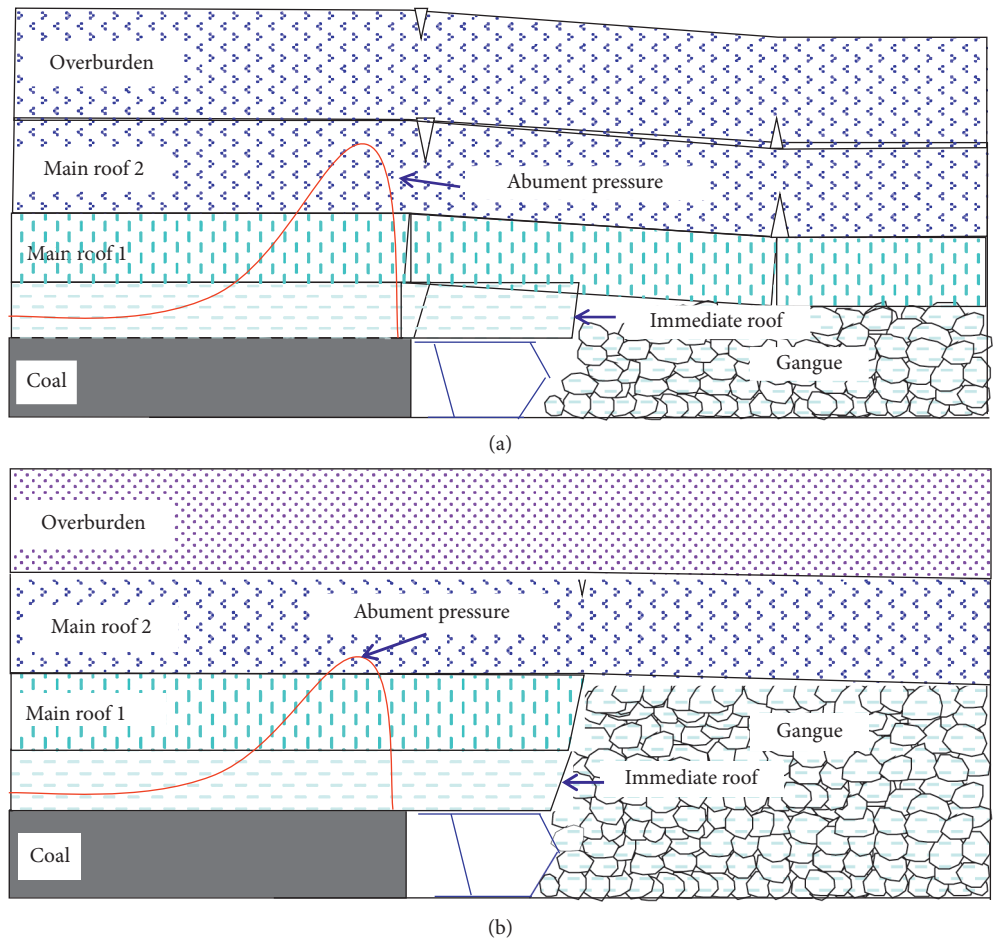

Figure 3: The structural model after overlying strata in goaf stabilize. (a) Conventional mining conditions. (b) Dual pressure relief.

$$p_2(x) = k_2 e^{\beta_2 x}\left(\frac{\beta_2 - \beta_1}{\beta_1 + \beta_2}\sin\beta_2 x + \cos\beta_2 x\right)\cdot\left(\frac{q_0}{k_1} + H_G - H_{c1}(k-1) - \Delta H\right)\cdot\frac{\beta_1^2}{\beta_2^2} + q_0. \quad (8)$$

According to formula (8), pressure p_2 on coal ahead of the working face decreases with the growth of the caving height H_{c1} of the immediate roof on premise of ignoring the influence of floor heave in goaf and keeping the mining height of the working face unchanged. The blasting-based roof cutting is equivalent to an artificial increase in the caving height H_{c1} of the immediate roof. Thus, it is possible to reduce the abutment pressure p_2 of coal ahead of the working face, thus decreasing the accumulation of energy in the working face and preventing a rockburst.

2.2. Directional Presplitting Blasting. As one type of presplitting blasting, directional presplitting blasting differs from traditional presplitting blasting. It changes the dynamic process of the interaction between detonation waves and surrounding rocks through effective combination of binding energy tubes and ordinary mining explosives. That is, the tangent tensile stress is formed along the direction of cumulative explosion after ignition. The detonation pressure is transformed into the tensile effect on surrounding rocks to the maximum extent, thus forming an effective fracture surface along the axial direction of roadways [30].

The model for a binding energy tube is demonstrated in Figure 5: holes and slots for cumulative explosion are linearly distributed on the left-hand and right-hand sides of the binding energy tube. After explosives in the binding energy tube are ignited, the tube will curb the propagation of the detonation products. The holes for cumulative explosion linearly distributed in the two sides of the binding energy tube offer the space for pressure relief of the detonation products. As a result, high-energy flows are formed at the holes and affect the hole wall, thus resulting in the generation of initial cracks in the rock mass.

Thereafter, the high-temperature, high-pressure, and high-speed gases generated due to detonation are still preferentially released from the holes for cumulative explosion following the detonation in the early period. Moreover, they rapidly propagate along the extension direction of the binding energy tube under the guidance of the slots for cumulative explosion to form air wedges, driving the extension and coalescence of radial initial cracks

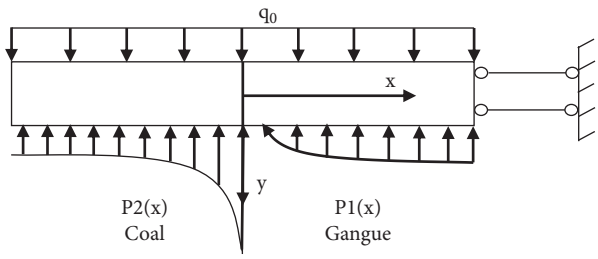

Figure 4: Stress diagram of the main roof 2 after making contact with gangues.

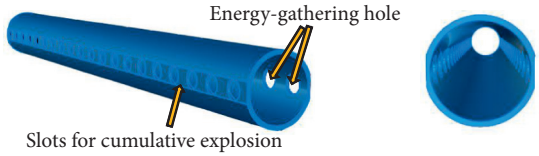

Figure 5: The model for a binding energy tube.

(Figure 6). Additionally, the detonation products impact the blast hole walls to generate explosion-induced stress waves. Furthermore, compressive stress is generated in the rocks in the radial direction of the blast holes, while a concomitant tensile stress is formed in the circumferential direction. As the tensile strength of rocks is much smaller than the compressive strength, rocks are fractured under the effect of circumferential tensile stress to form the radial fractures, thus forming an effective fracture surface along such roadways [31, 32].

3. Analysis of the Outburst-Control Effect

3.1. Engineering Situation. The test was conducted based on the 513 working face of Longjiapu Coal Mine located in Changchun, Jilin Province, China. The working face is located on the south wing of No. 5 mining area, and it lies adjacent to the 411 working face. The working face is at a burial depth of 1073.3 to 1215.8 m, with a strike length of 600 m and a dip length of 182 m. The coal seam in the working face has a thickness of 8 to 12 m, with an average thickness of 10 m; the dip angle of the coal seam is between 10° and 20°, with an average dip angle of 15°. The working face was mined by using fully mechanized coal caving mining, with a height of coal cutting of 3 m, and the height of coal discharge is 7 m. The overlying strata are siltstone with a thickness of 17.1 m, fine sandstone with a thickness of 6.3 m, and siltstone with a thickness of 31.9 m. The floor of the coal seam in the working face comprises tuffaceous siltstone (1.3 m thick) and siltstone (10.1 m thick). The basic conditions at the working face are shown in Figure 7.

The dual pressure relief scheme for the working face was designed according to the geological and mining characteristics of the 513 working face, as shown in Figure 8. The specific parameters are listed as follows: (1) the position of roof cutting is located in the roadway side in the side of the working face within the conveyor gateway and return airway, which is 3 m above the roadway floor; (2) the presplit cut has a depth of 18 m. The boreholes for cutting having an included angle of 10° with the vertical direction were inclined to the side of the working face and the spacing between adjacent boreholes was 0.5 m; (3) the sealing length was 2.25 m and 10.5 binding energy tubes were placed into each blasting borehole. The numbers of cartridges outwards from the boreholes are, separately, 4 + 4 + 4 + 4 + 3 + 3 + 2 + 2 + 1 + 1 + 0; and (4) the explosives measured $\varphi 53 \times 200$ mm. A positive air-decoupling charge was applied, and explosives were initiated in no more than eight blasting boreholes each time.

3.2. Energy Distribution Characteristics in the Working Face under the Influence of Dual Pressure Relief

3.2.1. Establishment of a Numerical Calculation Model. According to the prevailing geological conditions in the Longjiapu Coal Mine, the 513 working face was simulated using FLAC3D. The model measured a simulated 290 m × 150 m × 210 m (length × width × height). The simulated working face has a dip length of 180 m and a strike length of 150 m. The constitutive model used was a Mohr-Coulomb model. Two conditions (with and without dual pressure relief) were simulated, as shown in Figure 9. The roof cutting was simulated by applying a null unit and the goaf near the position of roof cutting was backfilled based on the strain-hardening model. The working face was excavated for 85 m and the model was loaded in 3000 steps. The physicomechanical parameters of various strata are listed in Table 1.

3.2.2. Energy Distribution in the Working Face. The occurrence of a rockburst is fundamentally attributed to the release of energy stored in the coal; therefore, the energy distribution characteristics in coal ahead of the working face before and after implementation of dual pressure relief were compared. The density of the elastic strain energy refers to the elastic strain energy per unit volume of a material. It is supposed that the stresses on various surfaces of rock units increase to the final value from zero in the same proportion. The density of the elastic strain energy in rock units on the linear-elastic condition was calculated according to the following formula [33]:

$$U^e = \frac{1}{2E_a}\left[\sigma_1^2 + \sigma_2^2 + \sigma_3^2 - 2\mu\left(\sigma_1\sigma_2 + \sigma_2\sigma_3 + \sigma_1\sigma_3\right)\right], \quad (9)$$

where σ_1, σ_2, and σ_3 represent the maximum, intermediate, and minimum principle stresses; E_a, μ, and U^e separately denote the elastic modulus, Poisson's ratio, and the density of the elastic strain energy.

The density of the elastic strain energy in coal after mining the working face was determined according to formula (9). Moreover, the data pertaining to the energy density in coal ahead of the working face was extracted to draw a nephogram, with the range of data extraction in Figure 10.

Figure 11 shows the nephogram for the density of the elastic strain energy in coal ahead of the working face. It can be seen from Figure 11(a) that the density of the elastic strain

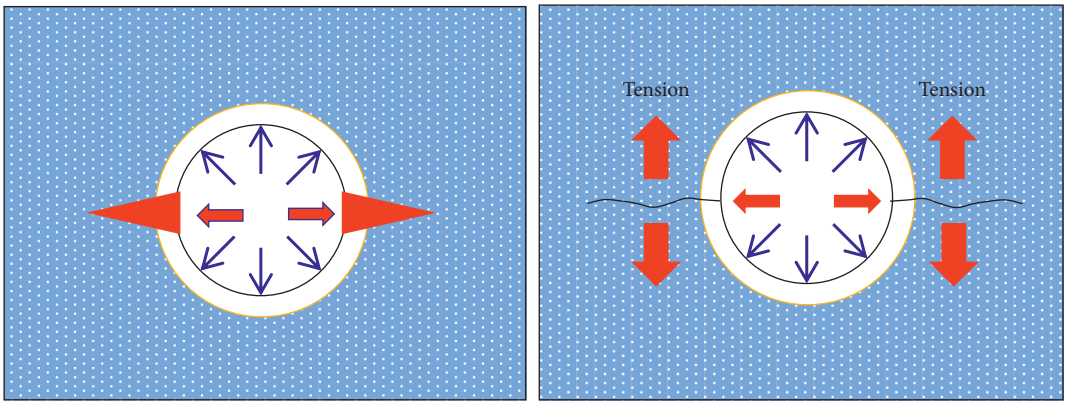

Figure 6: The working principle of a directional presplitting blasting.

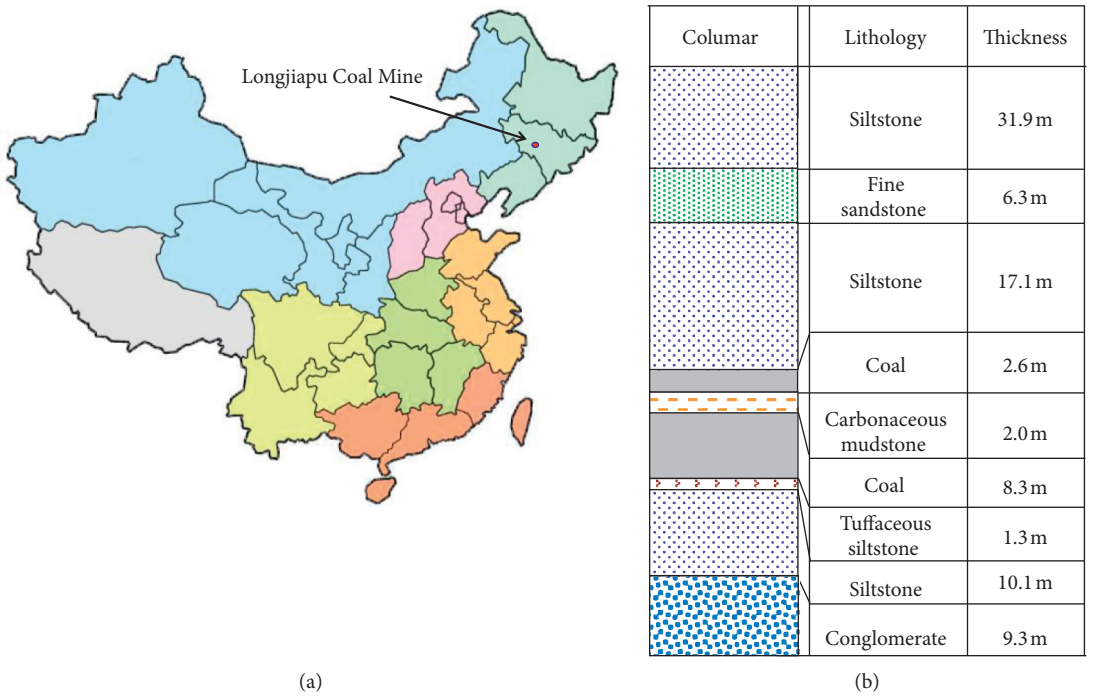

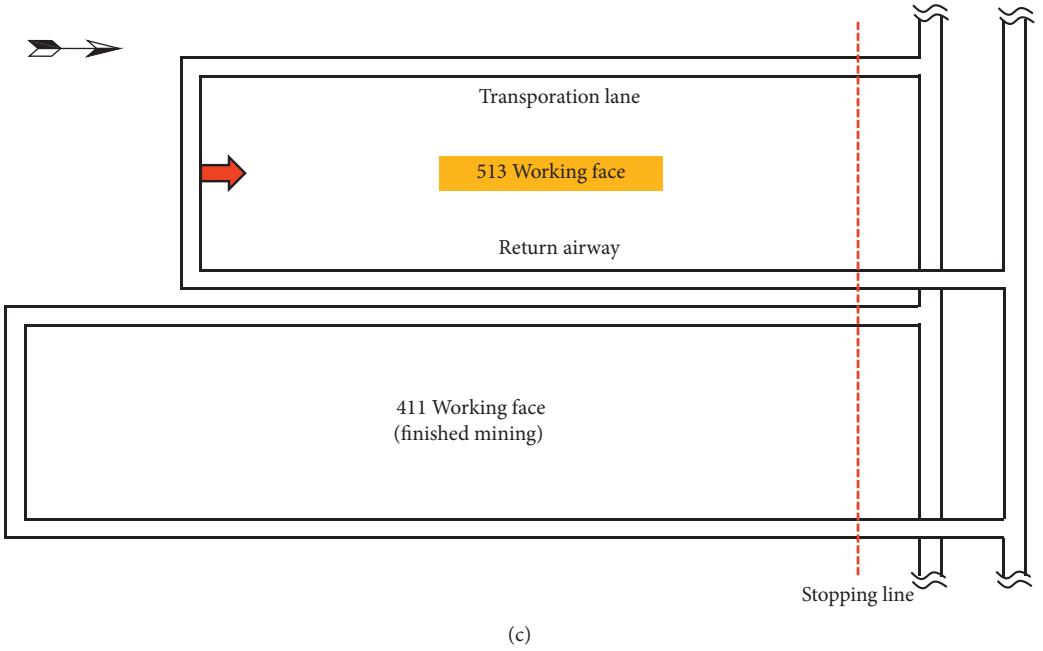

Figure 7: Engineering conditions. (a) Geological situation. (b) Geological column through the working face. (c) Working face layout.

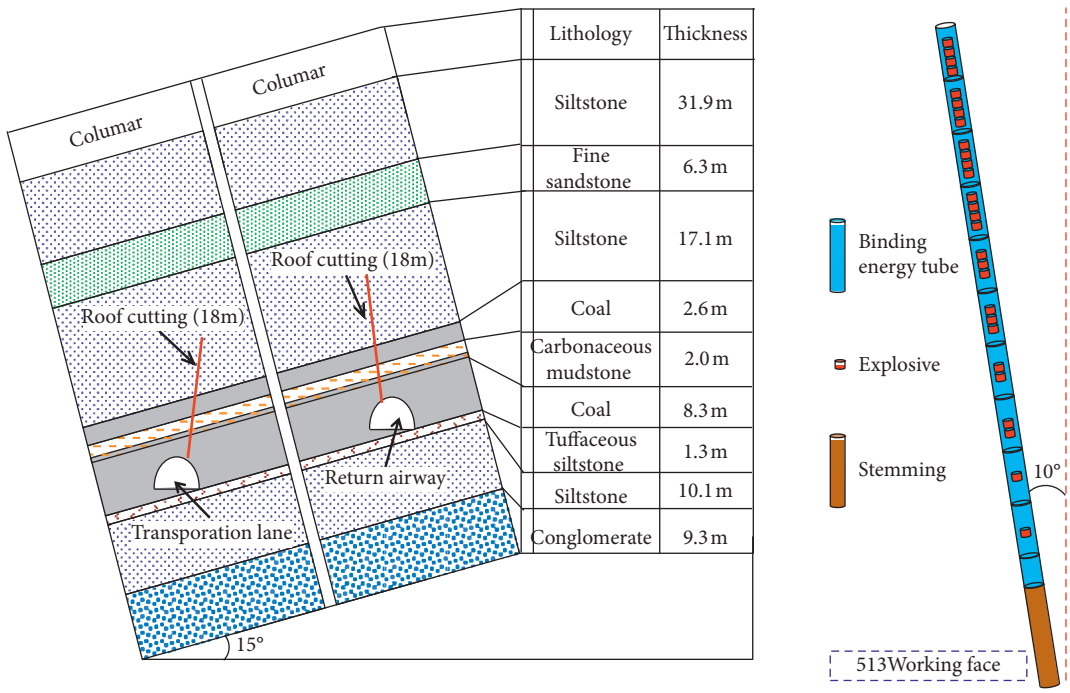

Figure 8: The dual pressure relief technology scheme and charge structure.

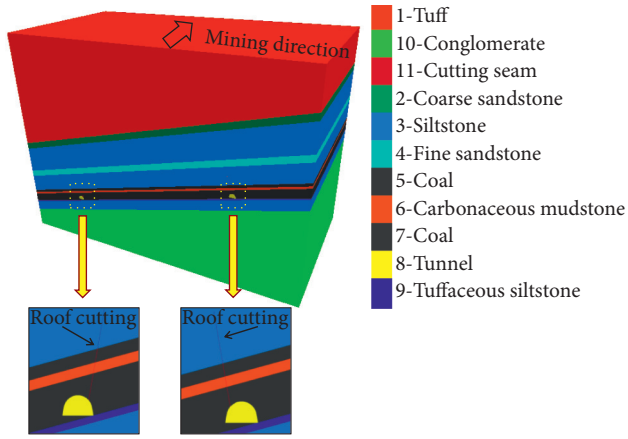

Figure 9: Numerical calculation model.

Table 1: Mechanical parameters of the model strata.

Lithology	Density (kg/m^3)	Tensile strength (MPa)	Friction angle (°)	Cohesion (MPa)	Bulk modulus (GPa)	Shear modulus (GPa)
Tuff	2240	2.38	36	2.7	2.76	1.3
Coarse sandstone	2560	1.50	34	5.0	4.2	2.9
Siltstone	2702	1.31	38	2.5	2.8	1.2
Fine stone	2873	1.29	24	3.2	2.1	1.35
Coal	1346	1.48	39	2.8	2.8	3.6
Carbonaceous mudstone	2891	1.15	29	1.3	2.17	1.0
Tuffaceous siltstone	2360	1.33	38	2.06	10.6	8.03
Conglomerate	2580	1.2	27	2.3	3.3	2.5

energy reaches a peak within a certain range in front of the working face under conventional mining conditions: this indicates that high strain energy was stored in rock within the range. By calculating the mean average of the densities of the elastic strain energy, the curve of the average energy density along the strike of the working face was obtained, as

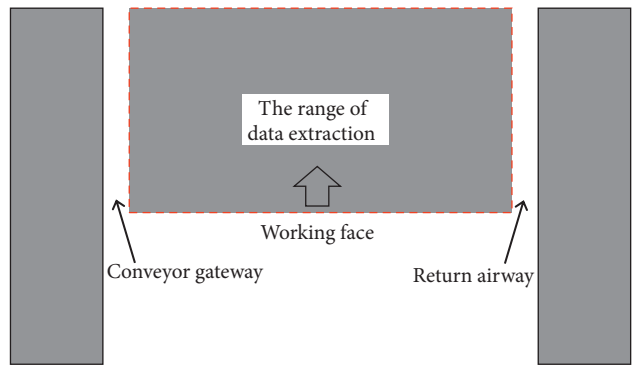

Figure 10: Extraction position of elastic strain energy.

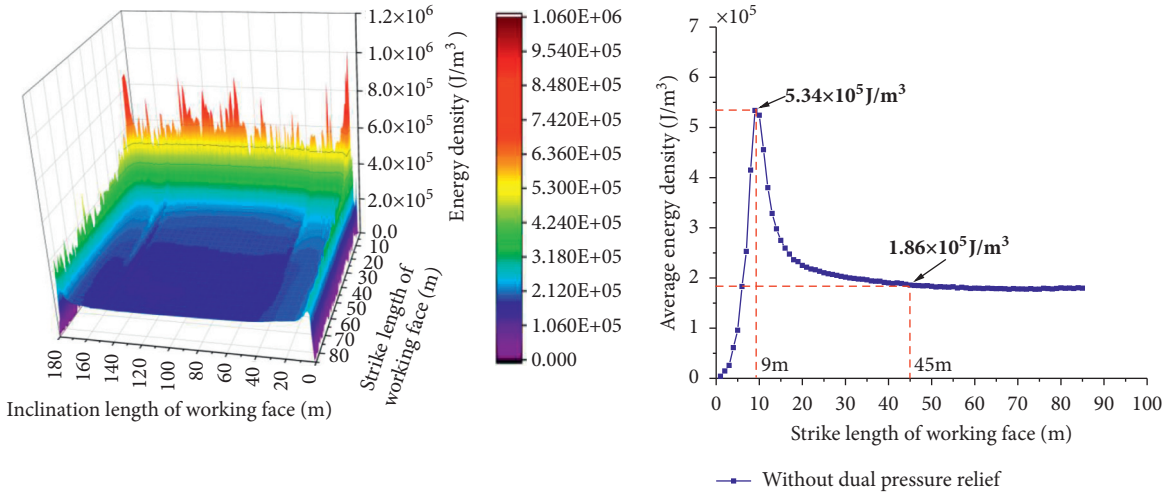

Figure 11: Distribution of energy density in the working face under conventional mining conditions. (a) Nephogram of energy density. (b) The average energy density.

shown in Figure 11(b). The average strain energy density gradually grows within the range of 0 to 9 m along the strike of the working face, reaches the maximum (5.34×10^5 J/m^3) at 9 m, and then gradually declines to 1.86×10^5 J/m^3 at 45 m in front of the working face. Beyond 45 m in front of the working face, the average strain energy density in coal remains at about 1.86×10^5 J/m^3 and does not significantly vary thereafter. It can be found that the energy stored in coal within the range of 0 to 45 m ahead of the mined working face significantly increases. Therefore, the risk of occurrence of a rockburst increases: the range of 0 to 45 m ahead of the working face is taken as an area with potential rockburst risk.

Figure 12 shows the density of the elastic strain energy in coal ahead of the working face under dual pressure relief conditions. According to the spatial distribution characteristics (Figure 12(a)) of the energy density, the peak energy density still appears within a certain range in front of the working face after undertaking dual pressure relief. The change of the average energy density along the strike of the working face was evaluated (Figure 12(b)). The average strain energy density was found to gradually increase within the range of 0 to 9 m along the strike of the working face after application of dual pressure relief, reaching a maximum (5.05×10^5 J/m^3) at 9 m and then gradually reducing to 1.86×10^5 J/m^3 at some 45 m ahead of the working face. Beyond that point, the average strain energy density in the coal remains at 1.86×10^5 J/m^3.

Figure 13(a) shows the curves of the average energy density along the strike of the working face before and after dual pressure relief. As shown in Figure 13(a), the strain energy density in coal within the range of 20 m along the strike of the working face is obviously weakened by using the dual pressure relief method. The change of the average energy density in coal within the range of 20 m along the strike of the working face was assessed. The density of the elastic strain energy in coal along the dip of the working face (within the range of 20 m along the strike of the working face) before and after dual pressure relief was thus derived as shown in Figure 13(b): the dual pressure relief method significantly weakens the strain energy density in the coal within the range of 30 m from the two roadways along the dip of the working face. The energy density in the side of the

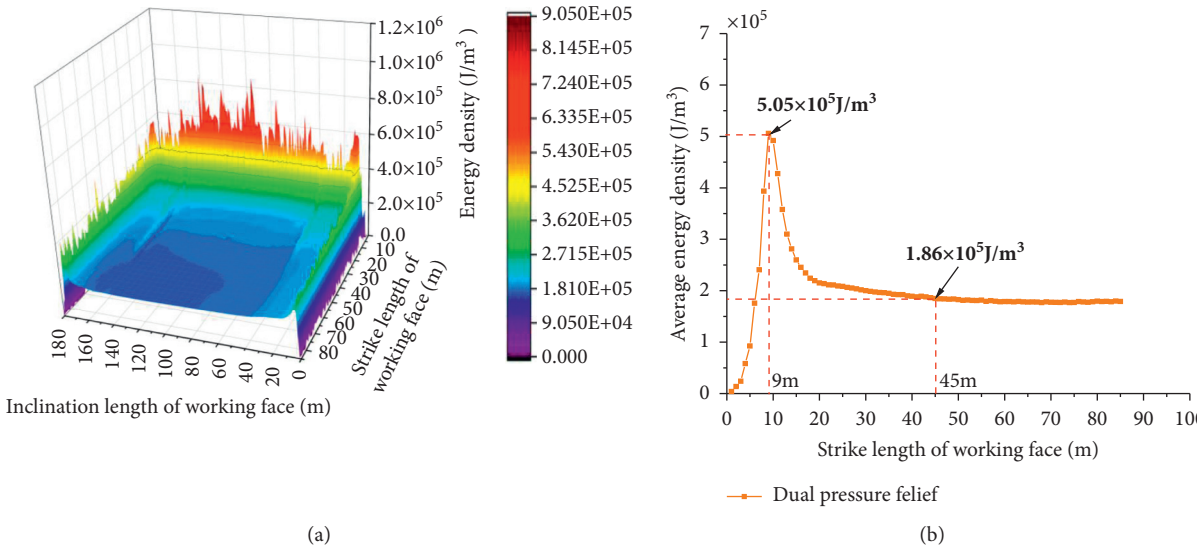

Figure 12: The distribution of the energy density in the working face after dual pressure relief. (a) Nephogram of energy density. (b) The average energy density.

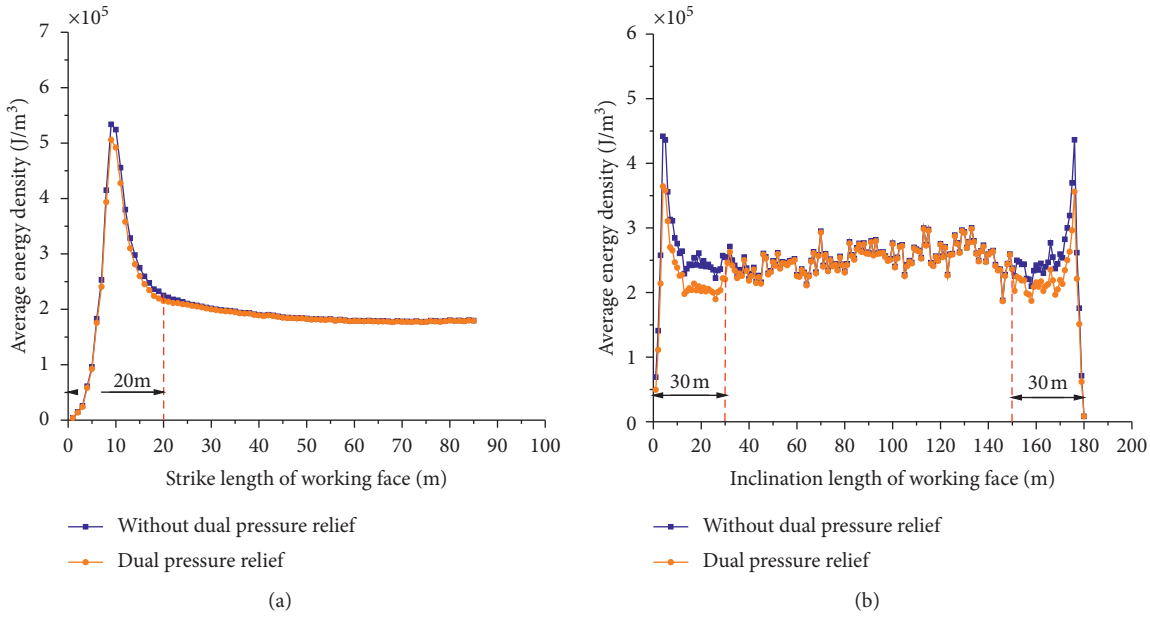

Figure 13: Comparison of the curves of average energy in coal ahead of the working face before and after dual pressure relief. (a) Along the strike of the working face. (b) Along the dip of the working face.

conveyor gateway is decreased by 15.4%, while that in the side of the return airway is decreased by 13.8% compared with the situation before implementation of pressure relief.

3.3. Stratal Behaviors during Mining of the Working Face under the Influence of Dual Pressure Relief. To investigate stratal behaviors in the working face after dual pressure relief, the daily average pressure data on the hydraulic supports of the working face were extracted. On this basis, the nephogram of the average pressure on supports and curves of pressure on supports at key locations during the mining were plotted, as shown in Figure 14. According to the nephogram of the mine pressure and curves of the working resistance on the supports, the stratal behaviors in the working face under the influence of dual pressure relief show the following characteristics:

(1) Low-pressure zones are found in two ends of the working face. As shown in Figure 14(a), the pressure on supports within the ranges of 0 to 30 m from the conveyor gateway and 0 to 25 m from the return airway remain low. The average pressures on supports within the range of 0 to 30 m from the conveyor

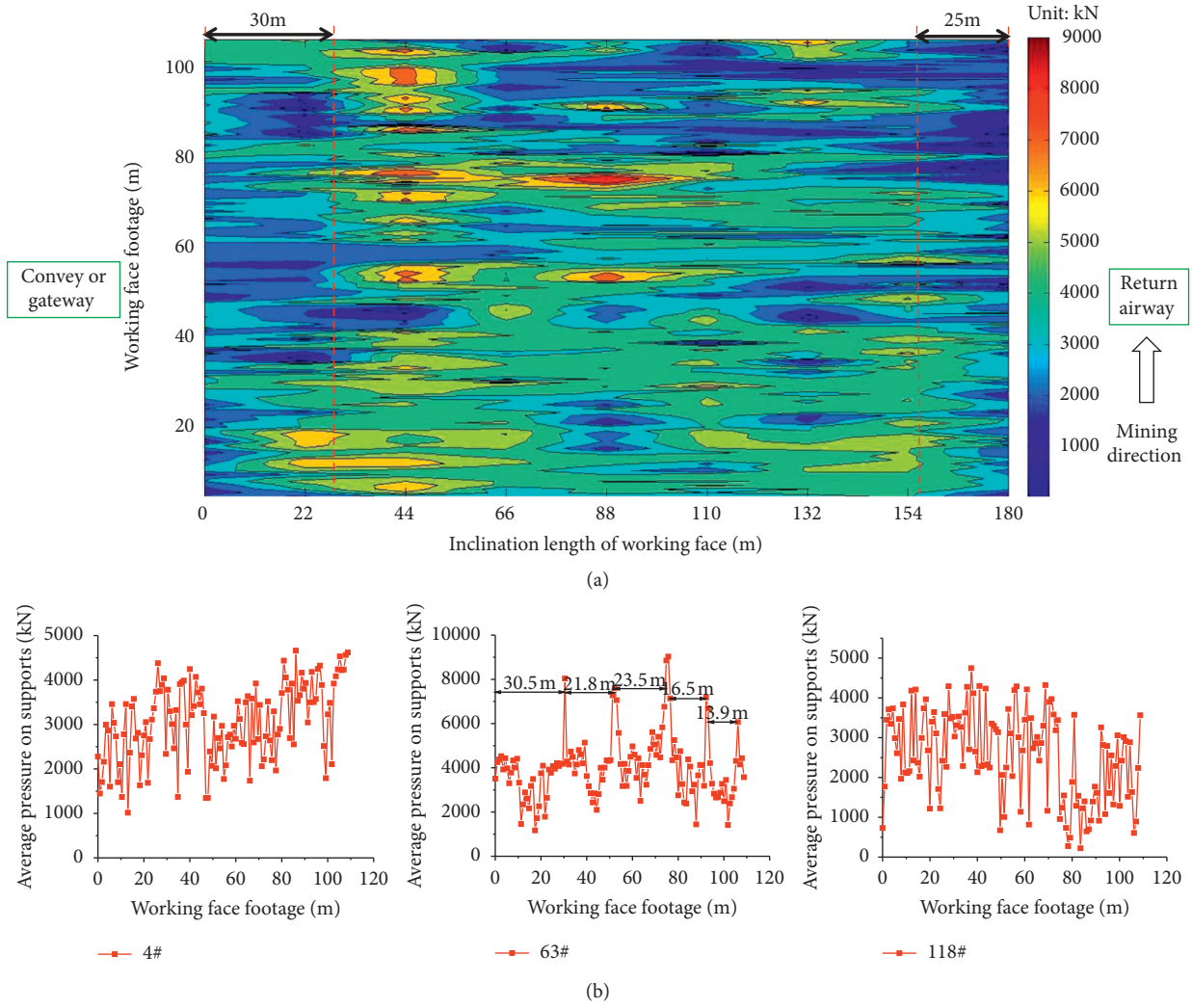

Figure 14: Characteristic maps of the pressure on supports in the 513 working face. (a) Nephogram of the mine pressure on the working face. (b) Working resistance of the supports.

gateway are 3265 kN, and the average pressure on supports within the range of 0 to 25 m from the return airway is 3299 kN. The average pressure on supports in the middle part of the working face is 4153 kN. Compared with the middle part of the working face, the pressure in the side of the conveyor gateway after dual pressure relief is decreased by 21.4%, while that in the side of the return airway reduces by 20.5%.

(2) The middle part of the working face suffers a high intensity of weighting, which shows obvious impact characteristics. In Figure 15(b), the 4# support is 6 m away from the transportation lane, the 4# support is located in the middle of the working face (94.5 m from the transport chute), and the 118# support is 3 m from the return airway. It can be seen from the pressure curve of the 63# support in Figure 14(b) that the periodic weighting in the middle part of the working face is significant. The intensity of the first weighting, the intensity of periodic weighting, and the average intensity of periodic weighting are 8040, 6067 to 9029, and 7469 kN, respectively, which are higher than the rated working resistance (7000 kN) of the supports. The pressure on the support in the working face increases significantly during the weighting, and the average increase in load is 3462 kN.

(3) The periodic weighting in the middle part of the working face exhibits a large step distance, with no obvious characteristics of periodic weighting in the low-pressure zones in two ends. As shown in Figure 14(b), the step distance of the first weighting, the step distance of periodic weighting, and the average step distance of periodic weighting in the middle part (63# support) of the working face within the advancement range of 110 m of the working face are 30.5, 13.9 to 23.5, and 18.9 m, respectively. No significant periodic weighting is present within the low-pressure zones (4# and 118# supports) at the two ends.

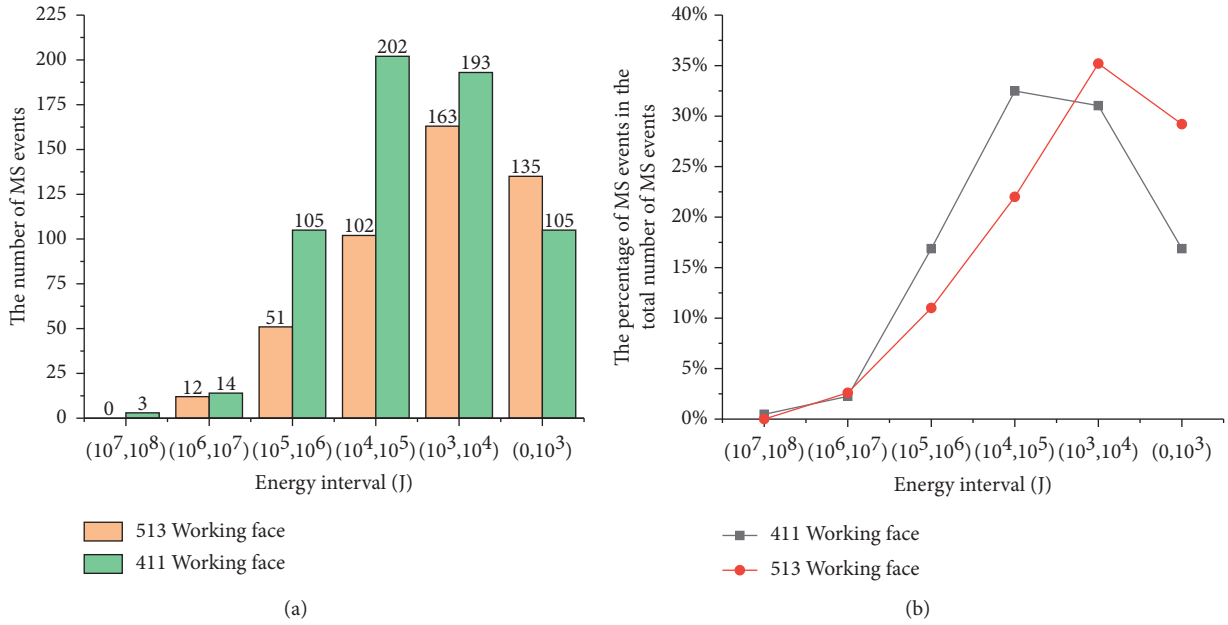

Figure 15: The number and proportion of MS events in different energy ranges before and after dual pressure relief. (a) The number of MS events. (b) The proportion of MS events in different energy ranges.

Overall, dual pressure relief reduces the pressure on supports within the range of 30 m from the conveyor gateway and the range of 25 m from the return airway and eliminates the periodic weighting caused by sudden fracture of the hard roof.

3.4. Energy Release during Mining of the Working Face under the Effect of Dual Pressure Relief. The occurrence of MS events is a real-time response to the energy release during mining; therefore, the MS characteristics of the 513 working face during the dual pressure relief and those of its adjacent working face (the 411 working face with no use of dual pressure relief) were compared. The positional relationship between the 513 working face and the 411 working face is shown in Figure 7(c). On this basis, the influence of dual pressure relief in the stope on rockburst risk was assessed.

According to the field monitoring results, the MS events with energies of the order of magnitude of up to 10^7 J mainly occurred during the mining of the 513 and 411 working faces. Therefore, the number and proportion of MS events within the energy range were calculated and their curves were plotted, as shown in Figure 15: a total of 622 MS events occurred in the 411 working face before dual pressure relief, of which 32.5% and 31% occurred separately within the ranges of [10^4, 10^5) and [10^3, 10^4) J. The numbers of MS events within the ranges of [0, 10^3) and [10^5, 10^6) J both accounted for 16.9%. A total of 464 MS events arose in the 513 working face after pressure relief, of which 35.2%, 29.2%, 22%, and 11% are separately in the ranges of [10^3, 10^4), [0, 10^3), [10^4, 10^5), and [10^5, 10^6) J.

Table 2 lists the statistical results of the changing MS events before and after implementation of pressure relief. According to Table 2 and Figure 15, the total number of MS events during the mining of the working face after dual pressure relief declines by 25.4%. The numbers of MS events within the ranges of [10^5, 10^6), [10^4, 10^5), [10^3, 10^4), and [10^6, 10^7) J are decreased by 51.4%, 49.5%, 15.5%, and 14.3%, respectively. By contrast, the number of MS events with an energy no greater than 10^3 increases by 28.6%. Additionally, MS events with an energy no lower than 10^7 J do not occur after pressure relief.

The use of dual pressure relief can decrease the MS energy release during the mining of the working face. The numbers of MS events in the energy ranges above and below 10^3 J separately decline by 36.6% and increase by 28.6%. This indicates that dual pressure relief weakens the total release of MS energy from the working face. In addition, it causes a change in the characteristics of MS energy release from coexistence of low-energy events and a small number of high-energy events to the occurrence of numerous low-energy events (this is conducive to the effective control of rockburst).

4. Discussion

4.1. The Differences in Stratal Behaviors within and beyond the Range of Influence of Dual Pressure Relief. The height of caved gangues filled in goaf is regarded as the key influencing factor restricting the subsidence of overlying strata towards goaf, which is directly associated with the roof-cutting height. When the roof-cutting height is sufficiently large, the gangues caved into goaf can backfill the goaf, restricting movement of the overlying strata after being broken. As a result, the overlying strata of goaf suffered less bending and subsidence and they remained unfractured before stabilization. Therefore, the pressure on the supports declines and the periodic weighting disappears from the working face within the range of influence of the applied dual pressure

Table 2: Changes in MS events within different energy ranges before and after dual pressure relief.

Energy range (J)	Number of MS events before pressure relief	Number of MS events after pressure relief	The number change of MS events before and after pressure relief	The percentage of the variation of MS events in the total number of MS events in corresponding energy ranges before pressure relief
$[10^7, 10^8)$	3	0	−3	−100
$[10^6, 10^7)$	14	12	−2	−14.3
$[10^5, 10^6)$	105	51	−54	−51.4
$[10^4, 10^5)$	202	102	−100	−49.5
$[10^3, 10^4)$	193	163	−30	−15.5
$[0, 10^3)$	105	135	30	28.6

Note: a negative number represents a reduction and a positive number represents an increase.

relief; by contrast, the caved gangues in goaf beyond that range are of small volume and they fail to backfill the goaf after being broken. Gangues do not significantly inhibit movement of the overlying strata. The roof of goaf bends and subsides as the working face is excavated and it is fractured after the subsidence reaches a certain extent: the pressure on supports in the working face decreases significantly, showing obvious periodic weighting.

4.2. The Mechanism of Energy Dissipation during Mining of the Working Face under the Influence of Dual Pressure Relief. In terms of the form of caving arising after dual pressure relief, it develops from bending and subsidence, local fractures, and fracturing to direct caving in some overlying strata, which eliminates the energy accumulation otherwise caused by bending and subsidence of the strata. In terms of rock with the same volume, more fractures are generated during caving than during fracturing. Thus, more energy is dissipated during fracturing of the rock and the change in mode of fracture causes a reduction in the number of high-energy events while increasing the number of low-energy events under dynamic load.

The inhibiting effect of gangues on movement of overlying strata weakens the subsidence and rate of subsidence of the overlying strata. Furthermore, it is possible to relieve the accumulation and rate of release of the elastic strain energy in strata and coal ahead of the working face and weaken the effect of dynamic loading on the movement of overlying strata on coal in the working face. This causes a decrease in the number of high-energy events occurring due to superposition of dynamic and static loads.

Additionally, gangue piles have a lower stiffness than coal and they can function as cushions to absorb the dynamic load transferred by fracture and movement of overlying strata or stress waves transferred during a mine earthquake. In this way, the impact-induced damage caused by the instability of overlying strata is relieved; therefore, the dual pressure relief technique can reduce the number of high-energy MS events during mining of the working face.

4.3. Advantages and Limitations. Compared with traditional pressure relief techniques, dual pressure relief does not transfer stress by weakening the coal rock. Instead, it fundamentally weakens the advanced abutment pressure of the working face by using the support effect of broken gangues on the roof of goaf. In addition, the surrounding rocks were only slightly damaged during blasting, thus avoiding the drawback present in the traditional pressure relief scheme; that is, the weakening of surrounding rocks caused a reduction in impact-resistance of the surrounding rocks. The proposed technique can therefore better prevent a rockburst.

It is noteworthy that this was the first attempt to apply dual pressure relief technology to actual rockburst control. During in situ testing, dual pressure relief was applied on the basis of traditional pressure relief measures, to good effect; therefore, it is necessary to combine the dual pressure relief technique with traditional pressure relief methods, thus guaranteeing the prevention of a rockburst as far as possible.

5. Conclusions

The mechanism of action of dual pressure relief in preventing rockbursts was studied from a theoretical perspective and the effect of the dual pressure relief method in controlling rockbursts was evaluated through numerical simulation and field testing. The results are as follows:

(1) A new method for controlling rockbursts through dual pressure relief by roof cutting through cumulative blasting in medium-deep holes conducted in the conveyor gateway and return airway was proposed. The mathematical relationship between the roof-cutting depth and the advanced abutment pressure of the working face was derived. The mechanism of action of dual pressure relief in preventing rockbursts was revealed.

(2) The results of numerical simulation showed that, as for the dual pressure relief method, the range of influence along the strike covers some 20 m in front of the working face, while that along the dip involves 30 m separately away from the two roadways. The energy density of coal within the range of influence in the side of the conveyor gateway decreases by 15.4%, while that in the side of the return airway decreases by 13.8% relative to those before pressure relief.

(3) The in situ monitoring indicated that the average support pressure within 30 m from the conveyor gateway reduces by 21.4%, while that within 25 m of the return airway decreases by 20.5% after implementing dual pressure relief. The periodic weighting

caused by fracturing of the hard roof within the range of influence of the dual pressure relief disappears.

(4) After applying dual pressure relief to alleviate the risk of a rockburst, the total number of MS events in the working face decreases by 25.4%. Those MS events with an energy release no lower than 10^7 J cease, and the numbers of MS events with energy release greater and smaller than 10^3 J separately decrease by 36.6% and increase by 28.6%. The energy released in MS events changes from a pattern of coexistence of low-energy events and a small number of high-energy events to the occurrence of numerous low-energy events.

Data Availability

The data used to support the findings of this study are available from the corresponding author upon request.

Conflicts of Interest

The authors declare that there are no conflicts of interest regarding the publication of this study.

Acknowledgments

This research was funded by the National Natural Science Foundation of China (nos. 52074300 and 52104139), the State Key Laboratory for Geomechanics and Deep Underground Engineering, China University of Mining and Technology, Beijing (no. SKLGDUEK2020), and the Coal Burst Research Center of China Jiangsu.

References

[1] T.-b. Zhao, W.-y. Guo, Y.-l. Tan, Y.-c. Yin, L.-s. Cai, and J.-f. Pan, "Case studies of rock bursts under complicated geological conditions during multi-seam mining at a depth of 800 m," *Rock Mechanics and Rock Engineering*, vol. 51, no. 5, pp. 1539–1564, 2018.

[2] W. J. Guo, Y. Y. Li, D. W. Yin, S. Zhang, and X. Sun, "Mechanisms of rock burst in hard and thick upper strata and rock-burst controlling technology," *Arabian Journal of Geosciences*, vol. 9, p. 561, 2016.

[3] Q. X. Qi, H. Y. Li, Z. G. Deng, S. K. Zhao, N. B. Zhang, and Z. W. Bi, "Studying of standard system and theory and technology of rock burst in domestic," *Coal Mining Technology*, vol. 22, no. 1, pp. 1–5, 2017.

[4] Q. X. Qi, H. Y. Li, S. K. Zhao et al., "Seventy years development of coal mine rockburst in China: establishment and consideration of theory and technology system," *Coal Science and Technology*, vol. 47, no. 9, pp. 1–40, 2019.

[5] P. K. Kaiser and M. Cai, "Design of rock support system under rockburst condition," *Journal of Rock Mechanics and Geotechnical Engineering*, vol. 4, no. 3, pp. 215–227, 2012.

[6] M. C. He, H. P. Xie, S. P. Peng, and Y. D. Jiang, "Study on rock mechanics in deep mining engineering," *Chinese Journal of Rock Mechanics and Engineering*, vol. 24, no. 16, pp. 2803–2813, 2005.

[7] Y. D. Jiang and Y. X. Zhao, "State of the art: investigation on mechanism, forecast and control of coal bumps in China," *Chinese Journal of Rock Mechanics and Engineering*, vol. 34, no. 11, pp. 2188–2204, 2015.

[8] Y. Z. Wu, Y. K. Fu, J. He, J. Chen, X. Chu, and X. Meng, "Principle and technology of "pressure relief-support-protectioncollaborative prevention" and control in deep rock burst roadway," *Journal of China Coal Society*, vol. 46, no. 1, pp. 132–144, 2021.

[9] J. F. Pan, Y. Ning, Z. H. Qin, S. Wang, and Y. Xia, "Dredging technology of pressure with deep-hole interval blasting based on theory of rock burst start-up," *Chinese Journal of Rock Mechanics and Engineering*, vol. 31, no. 7, pp. 1414–1421, 2012.

[10] M. T. Zhang, W. Y. Song, and Y. S. Pan, "Study on water pouring into coal seam to prevent rock-burst," *China Safety Science Journal*, vol. 13, no. 10, pp. 69–72, 2003.

[11] Q. X. Qi, Y. Lei, H. Y. Li, Z. W. Ji, and Y. X. Wang, "Theory and application of prevention of rock burst by break-tip blast in deep hole," *Chinese Journal of Rock Mechanics and Engineering*, vol. 26, no. S1, pp. 3522–3527, 2007.

[12] L. Y. Pan, H. Wei, L. Q. Chen, D. Y. Duan, and H. J. Liu, "Mechanism and application of using engineering defect to prevent and control rock burst," *Chinese Journal of Geotechnical Engineering*, vol. 39, no. 1, pp. 56–61, 2017.

[13] F. X. Jiang, B. Wang, M. H. Zhai, and J. R. Huang, "Field tests on fixed-point hydraulic fracture with extra-high pressure in coal seam for rock burst prevention," *Chinese Journal of Geotechnical Engineering*, vol. 37, no. 3, pp. 526–531, 2015.

[14] Z. H. Ouyang, Q. X. Qi, Y. Zhang, X. Z. Wei, and S. K. Zhao, "Mechanism and experiment of hydraulic fracturing in rock burst prevention," *Journal of China Coal Society*, vol. 36, no. S2, pp. 321–325, 2011.

[15] Y. X. Xia, W. J. Ju, and S. J. Su, "Experimental study on hydraulic reaming of gutters in coal seam with impact pressure," *Journal of Mining and Strata Control Engineering*, vol. 2, no. 1, pp. 1–8, 2020.

[16] Z. L. Li, X. Q. He, and L. M. Dou, "Control measures and practice for rockburst tinduced by over burden fracture in top-coal caving mining," *Journal of China University of Mining and Technology*, vol. 47, no. 1, pp. 162–171, 2018.

[17] S. K. Zhao, L. Y. Li, B. Y. Wu, and Z. G. Deng, "Theory and application of deep hole floor-break blasting in floor rock burst coal mine," *Journal of Mining and Safety Engineering*, vol. 33, no. 4, pp. 636–642, 2016.

[18] L. M. Dou, J. Z. Bai, X. W. Li, and H. He, "Study on prevention and control technology of rockburst disaster based on theory of dynamic and static combined load," *Coal Science and Technology*, vol. 46, no. 10, pp. 1–8, 2018.

[19] Z. H. Ouyang, "Application and mechanism of mine strata pressure pumping prevention with multi stage blasting pressure releasing technology," *Coal Science and Technology*, vol. 42, no. 10, pp. 32–74, 2014.

[20] J. H. Liu, W. L. Yang, F. X. Jiang, and X. S. Guo, "Mechanism of cracking-before-injecting method to prevent coal burst and its field test," *Chinese Journal of Rock Mechanics and Engineering*, vol. 36, no. 12, pp. 3040–3049, 2017.

[21] J. F. Pan, S. H. Liu, J. M. Gao, X. Sun, Y. Xia, and Q. Wang, "Prevention theory and technology of rock burst with distinguish dynamic and static load sources in deep mine roadway," *Journal of China Coal Society*, vol. 45, no. 5, pp. 1607–1613, 2020.

[22] C. C. Xue, A. Y. Cao, F. W. Niu, X. Wang, Z. Shen, and K. Tang, "Mechanism and prevention of rock burst in deep irregular isolated coal pillar," *Journal of Mining and Safety Engineering*, vol. 38, no. 3, pp. 479–486, 2021.

[23] J. Z. Yang and K. G. Zheng, "The mechanism of overburden dynamic disasters and its control technology in top-coal caving in the mining of thick coal seams," *Journal of Mining and Safety Engineering*, vol. 37, no. 4, pp. 750–758, 2020.

[24] Y. Chen, D. Li, F. X. Jiang et al., "Prevention mechanism of rock burst in backfill mining in extra-thick coal seam with deep shaft," *Journal of Mining and Safety Engineering*, vol. 37, no. 5, pp. 969–976, 2020.

[25] S. T. Zhu, "Mechanism and prevention of rock burst in extra-thick coal seams mining," Doctoral dissertation, University of Science and Technology Beijing, Beijing, China, 2017.

[26] Z. L. Li, "Principle and application of rockburst control by weakening static and dynamic loading using top-coal caving in the mining of thick coal seams," Doctoral dissertation, China University of Mining and Technology, Xuzhou, China, 2016.

[27] J. M. Gao, J. F. Pan, T. T. Du, and Y. Yan, "Characteristics and prevention and control status quo of rock burst in north-eastern mining area of China," *Coal Science and Technology*, vol. 49, no. 3, pp. 1–8, 2018.

[28] Z. Q. Song, *Practical Method of Mine Pressure Control*, pp. 87-88, China University of mining and Technology Press, Xuzhou, China, 1988.

[29] Y. L. Mo, H. Y. Li, Z. G. Deng, Q. X. Qi, H. T. Li, and G. H. Zhang, "Initial damage effect of energy response for coal with different bump proneness," *Journal of Mining and Safety Engineering*, vol. 37, no. 6, pp. 1205–1212, 2020.

[30] M. C. He, P. F. Guo, X. H. Zhang, and J. Wang, "Directional presplitting of roadway roof based on bidirectional shaped sharge tension blasting theory," *Explosion and Shock Waves*, vol. 38, no. 4, pp. 795–803, 2018.

[31] M. C. He, W. F. Cao, R. L. Shan, and S. L. Wang, "New blasting technology-bilateral cumulative tensile explosion," *Chinese Journal of Rock Mechanics and Engineering*, vol. 22, no. 12, pp. 2047–2032, 2003.

[32] X. Y. Zhang, J. Z. Hu, H. J. Xue et al., "Innovative approach based on roof cutting by energy-gathering blasting for protecting roadways in coal mines," *Tunnelling and Underground Space Technology*, vol. 99, pp. 1–12, 2020.

[33] H. P. Xie, J. Yang, and L. Y. Li, "Criteria for strengthand structural failure of rocks based on energy dissipationand energy release principles," *Chinese Journal of Rock Mechanics and Engineering*, vol. 24, no. 17, pp. 3003–3010, 2005.